Progress in Organic Coatings 188 (2024) 108229

Contents lists available at ScienceDirect

Progress in Organic Coatings

journal homepage: www.elsevier.com/locate/porgcoat

UV-curable acrylic end-capped amphoteric waterborne polyurethane coatings

M. Puyadena [a], E. Pajares [a], L. Martin [b], A. Barrio [c], A. González [a], L. Irusta [a,*]

[a] POLYMAT, Department of Polymers and Advanced Materials: Physics, Chemistry and Technology, University of the Basque Country UPV/EHU, PO Box 1072, 20080 Donostia-San Sebastián, Spain
[b] Macrobehaviour-Mesostructure-Nanotechnology SGIker Service, Faculty of Engineering, University of the Basque Country UPV/EHU, Plaza Europa 1, 20018 Donostia-San Sebastián, Spain
[c] TECNALIA, Basque Research and Technology Alliance (BRTA), Area Anardi 5, 20730 Azpeitia, Spain

ARTICLE INFO

Keywords:
UV curable acrylic end-capped waterborne polyurethanes
Amphoteric stabilisation
Dispersion stability

ABSTRACT

Waterborne polyurethane dispersions (WPUs) are environmentally friendly coatings since they present low amount of volatile organic compound amounts (VOCs). In the majority of the WPUs the dispersions are balanced with anionic groups and accordingly their stability at low pH is limited. In order to this drawback to be solved, in this work a tertiary amine containing chain extender (triethanolamine, TEOA) was introduced together with a conventional internal emulsifier (carboxylic acid) in acrylic end-capped polyurethane dispersions giving rise to amphoteric UV curable WPUs. After adding a radical photo-initiator and film formation, the coatings were cured under UV irradiation. The properties of amphoteric and anionic dispersions were compared. The best properties were obtained for the samples containing a 1/1 amine/acid molar ratio. Thus, while the anionic dispersions coagulated at low pH values, the 1/1 amphoteric dispersion showed high stability to pH changes. After curing this sample with UV irradiation, the gel content of the film was higher and the water vapour transmission rate was lower than that of the anionic polyurethane because of the strong acid/base interaction. The results showed that the amphoteric WPUs are promising for various applications, offering stability over a wider pH range than traditional formulations.

1. Introduction

Due to environmental concerns, Waterborne Polyurethane Dispersions (WPU) are increasingly replacing solvent-based formulations [1,2]. WPUs can be considered environmentally friendly compounds since they do not contain volatile organic compounds (VOCs) and therefore they can be used as green coatings and adhesives [3].

Like the vast majority of commercial polyurethanes, WPU dispersions are obtained by the polyaddition reaction between polyisocyanates and polyols that renders urethane groups [4]. However, it is well known that isocyanate groups are highly reactive towards water molecules, and accordingly to obtain WPUs different strategies such as the mini-emulsion polymerisation [5], the prepolymer process [6] and the acetone process [7,8] have been developed.

The prepolymer and the acetone processes are the most employed strategies to obtain WPUs. In these two methods, the dispersion is obtained in different steps, and they present similar characteristics [2]. In the first step, the polyurethane is prepared using a polyisocyanate, a polyol, and an internal emulsifier (that will stabilise the dispersion). In the acetone process to reduce the viscosity, the first step takes place in a low boiling point solvent (usually acetone) while in the prepolymer process the viscosity is controlled by reducing the molecular weight of the polyurethane. In the second step, in both methodologies water is added to the system, and consequently, polymer particles are generated. Afterwards in the prepolymer process, the reaction proceeds *via* a chain extension with a diamine. However, in the acetone process, the last step involves solvent removal under vacuum yielding the final VOC-free dispersion.

For a WPU dispersion with good colloidal stability to be obtained, the internal emulsifier is a key factor that allows the emulsification process at low shear rates. Although alcohols containing ionic and non-ionic groups can be used as stabilising agents [9] the majority of WPUs contain ionic type internal surfactants. Among the ionic surfactants, the anionic groups (mainly carboxylate groups) are preferred. Thus, the 2,2-

* Corresponding author.
E-mail address: lourdes.irusta@ehu.eus (L. Irusta).

https://doi.org/10.1016/j.porgcoat.2024.108229
Received 19 November 2023; Received in revised form 26 December 2023; Accepted 4 January 2024
Available online 15 January 2024

bis(hydroxymethyl)propionic acid (DMPA) is the most employed internal surfactant in the WPU synthesis.

However, due to the presence of the internal emulsifier WPUs present lower water resistance than their solvent-based counterparts. The cross-linking of the films is a common strategy to reduce the water sensitivity of the WPUs. Thus, cross-linking can be induced *via* sol-gel reaction [10,11] and also *via* acrylic end groups [12,13]. Another drawback of the ionically stabilised WPUs is their low stability against electrolytes [2]. The ionic polyurethane particles are stabilised because of the ionic double layer generated between the functionalised diol linked to the polyurethane and the counterion that is located in the water phase. Consequently, if the pH of the dispersion is changed (for example because of the introduction of an additive) the polyurethane particles coagulate.

One possible solution to reduce this effect is the introduction of amphoteric groups in the structure of the polyurethane [14,15]. In these systems, as they present both anionic and cationic groups, the change of the pH produces a rearrangement of the polyurethane particles that avoids the undesired coagulation of the system. However, although the amphoteric dispersions could present better properties than anionic or cationic ones the reports about these systems are scarcely found in the open literature. Thus, in some papers, zwitterionic polyurethanes containing sulphobetaine have been prepared to give antifouling [16,17] and self-healing solvent-based coatings [18]. Amphoteric hydrogels have also been prepared by mixing waterborne polyurethane with an acrylic emulsion to obtain multifunctional sensors [19]. Finally, some authors reported the synthesis of amphoteric polyurethane dispersions including carboxylic acid and tertiary amine groups in the polymer structure [20,21].

As expected, the introduction of amphoteric units increases the stability of the dispersions. However, to the best of our knowledge, no report has been done about the introduction of amphoteric groups in UV-curable waterborne polyurethane dispersions. Accordingly, the main goal of the present study was to prepare these types of dispersions and compare the behaviour with the conventional anionic-based ones.

2. Experimental

2.1. Materials

IPDI (isophorone diisocyanate, Sigma-Aldrich; 98 %), PCL (polycaprolactone diol, Sigma-Aldrich; Mn ~ 2000 g·mol^{-1}), DMPA (2,2-bis (hydroxymethyl)propionic acid, Sigma-Aldrich; 98 %), TEA (triethylamine, Sigma-Aldrich; ≥99 %), TEOA (triethanolamine, Panreac; 99 %), DBTDL (dibutyltin dilaurate, Sigma-Aldrich; 95 %), HEMA (2-hydroxyethyl methacrylate, Sigma-Aldrich; 97 %), 1-HCHPK (1-hydroxycyclohexyl phenyl ketone, Sigma-Aldrich), acetone (Sigma-Aldrich, ≥99.8 %), deionised water (Quimibacter, <1 μS·cm^{-1}), THF (tetrahydrofuran, Oppac; 99.9 %), DMF (dimethyl formamide, Sigma-Aldrich; ≥99.9 %), HCl (hydrochloric acid, Panreac; 37 %) and NaOH (sodium hydroxide, Sigma-Aldrich; 99.99 %) were employed as received.

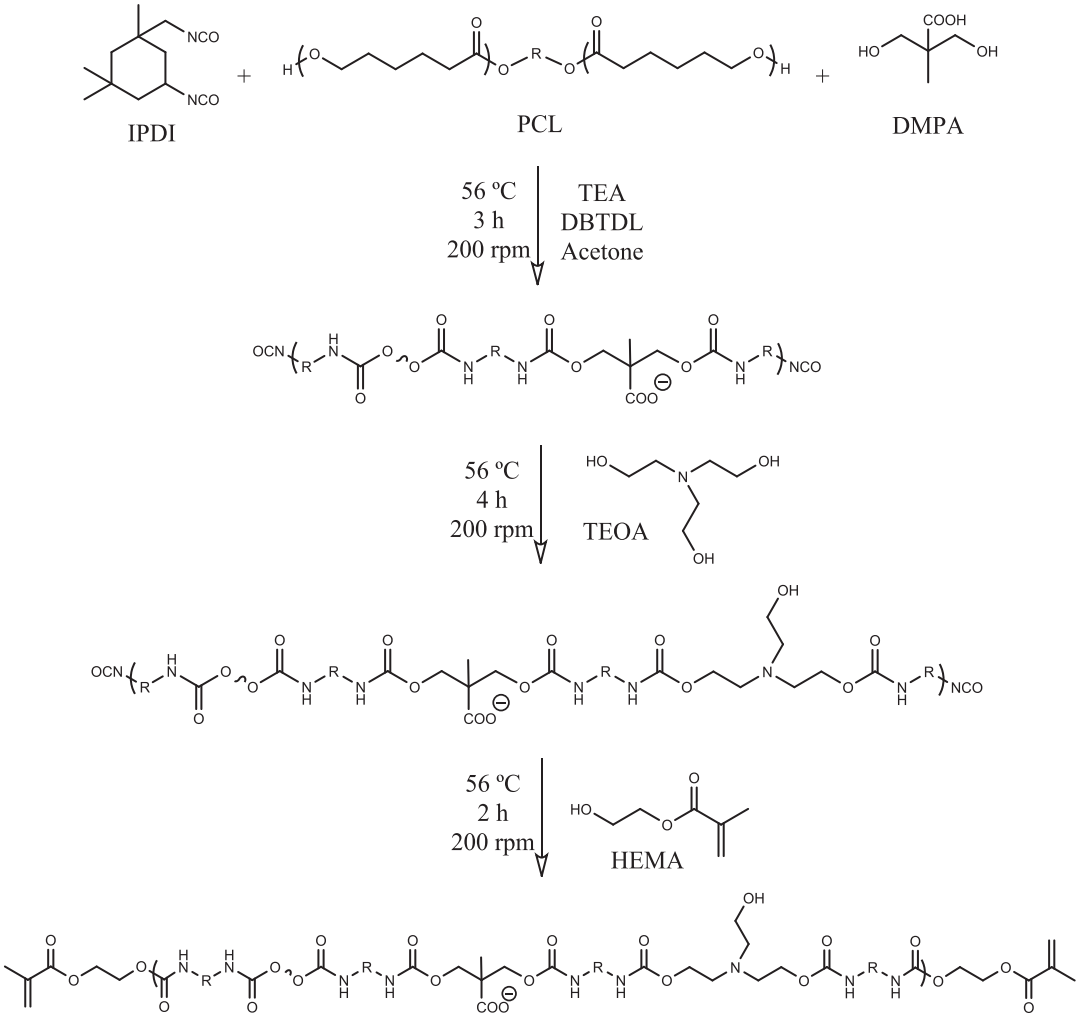

Scheme 1. Synthesis of the polyurethane prepolymer by acetone process.

2.2. Synthesis of PU

Waterborne polyurethane dispersions were synthesised through the acetone process as described in Scheme 1.

First, the diisocyanate (IPDI), the diol (PCL), and the internal emulsifier (DMPA) were placed in a jacked reactor attached to a water bath and were mechanically stirred at 200 rpm for 3 h at 56 °C. Acetone (40 wt% of the final polymer) was used as a solvent, a base (TEA, 105 mol% of DMPA) was employed to neutralise the DMPA acid groups, and a catalyst (DBTDL, 1 wt% of the final polymer) for increasing the reaction rate. Afterwards, TEOA was introduced into the medium when it was concerned and the reaction continued for another 4 h. The final polyurethane prepolymer was obtained once it was reacted with HEMA for further 2 h. In order to avoid the sample crosslinking, TEOA was considered as difunctional when calculating the reaction stoichiometry.

Subsequently, the reactor was cooled down to 25 °C, and water was added at 200 rpm producing the phase inversion. The amount of water was calculated to obtain dispersions with a final solid content of 30 wt%. Water based dispersions were obtained after acetone removal by a rotary evaporator under vacuum (100 mbar) at 30 °C for 1 h.

The amount of reagents employed for each synthesis is summarised in Table 1. Noteworthy, the samples were named according to the proportion of diol substituted by TEOA.

Crosslinked films for the gel content, DMA, WVTR and TGA measurements were obtained as follows. 25 g of the final dispersion was mixed with the corresponding amount of UV sensitive initiator (1-HCHPK) (0.5 wt%: 0.0375 g, 1 wt%: 0.0750 g and 1.5 wt%: 0.1125 g) and were dried over Teflon molds for 1 week in a dark place at room temperature. After drying, the samples were irradiated with a UV source lamp (Vilber-Lourmat VL-6LC UV) at 254 nm with an intensity of 1 $mW{\cdot}cm^{-2}$ for 1 h for each side of the film. For the contact angle measurements 100 μm thick samples were applied over microscope slides and were left to dry for at least 3 days in a dark place at room temperature. The dried samples were irradiated with the same UV lamp for 30 min.

2.3. Measurements

The polyurethane reaction kinetics was followed on a Nicolet 6700-IR (Thermo Scientific) FTIR (Fourier-transform infrared) spectroscopy attached to an ATR (attenuated total reflectance) accessory from Specac MKII Golden Gate. The spectra were recorded at different polymerisation times in a 4000–600 cm^{-1} range with a resolution of 4 cm^{-1} and 10 scans. The conversion of the NCO groups was calculated using Eq. (1) [22].

$$\text{Conversion}\ (\%) = 100 - \left(100 \frac{\left(\frac{A_{2260}}{A_{3000}}\right)_t}{\left(\frac{A_{2260}}{A_{3000}}\right)_{t_0}} \right) \quad (1)$$

where A_{2260} is the area of the stretching band of the isocyanate group at 2260 cm^{-1} and A_{3000} is the area of the bands due to the stretching vibration of the methyl and methylene groups close to 3000 cm^{-1}.

Differential scanning calorimetry (DSC) measurements were performed on a DSC Q2000 from TA Instruments to analyse the thermal properties of the samples and to follow the photo-polymerisation reaction. The photo-DSC measurements were performed at 25 °C irradiating 20 mm^2 area samples for 5 min with a UV source lamp (Vilber-Lourmat VL-6LC UV) at 254 nm with a 1 $mW{\cdot}cm^{-2}$ intensity, resting for another 5 min and repeating this procedure three times. The first irradiation stage gave information about the polymerisation, the second one was to ensure that the reaction was completed and the last one was taken as baseline. Samples were prepared drying about 5–10 mg of the dispersion in a dark place for at least 3 days at room temperature. From the area under the exothermic peak, the reaction conversion and the polymerisation rate (Rp) were calculated with Eqs. (2) and (3) respectively. Where ΔH_t was the measured photo-polymerisation reaction enthalpy at time t. The theoretical reaction enthalpy (ΔH_0^{theor}) was calculated according to Eq. (4), where the employed methacrylate molar enthalpy was 54.4 $kJ{\cdot}mol^{-1}$ [23], the functionality (f) was 2 and the Mw^{theor} was the theoretical polymer molecular weight.

$$\text{Conversion} = \frac{\Delta H_t}{\Delta H_0^{theor}} \quad (2)$$

$$Rp = \frac{d(\text{conversion})}{dt} = \frac{(dH/dt)}{\Delta H_0^{theor}} \quad (3)$$

$$\Delta H_0^{theor} = \frac{54.4 \bullet f}{Mw^{theor}} \quad (4)$$

Conventional DSC measurements were carried out in the same calorimeter. Samples were heated from −80 °C to 150 °C at a heating rate of 10 $°C{\cdot}min^{-1}$ under nitrogen flow. Afterwards, samples were cooled as quickly as possible to −80 °C and a second heating scan was made in the same conditions as the first one. For the cross-linked polymers samples cured in the photo-DSC were used. The non-cured prepolymers were prepared drying the samples with the same procedure used in the photo-DSC experiments. The PCL crystallinity (Xc) was calculated by Eq. (5), where ΔH was the sample melting enthalpy, ΔH^0 the melting enthalpy of the 100 % crystalline PCL (135.44 $J{\cdot}g^{-1}$) [24] and PCL wt% the weight percentage of the PCL of the analysed sample.

$$Xc = \frac{\Delta H}{\Delta H^0 \bullet \text{PCL wt\%}} \quad (5)$$

Thermogravimetric analyses (TGA) were performed on a TGA Q500 from TA Instruments. Samples of about 5–25 mg were heated from 30 °C to 800 °C at a heating rate of 10 $°C{\cdot}min^{-1}$ and under a nitrogen flow of 90 $mL{\cdot}min^{-1}$.

z-Potential or electrokinetic potential measurements were carried out on a Malvern Zetasizer Ultra (Malvern Paralytical Instruments). The measurements were carried out as a function of pH by Zetasizer MPT-3 Multi-purpose Titrator (Malvern Paralytical Instruments). Using this analysis, the IEP (isoelectric point) and the particle size values as a function of the pH were calculated. Samples were diluted with distilled water (concentration of 0.5 $mg{\cdot}mL^{-1}$) and were sonicated for 1 h at room temperature. The measurements were performed on plastic zeta DTS1070 cuvettes, from pH 12 to 3, at a temperature of 25 °C and a backscatter angle of 175°. The pH values were adjusted using HCl (0.1 and 0.5 M) or NaOH (0.5 M) solutions.

Thermo Scientific size exclusion chromatography (SEC), fitted with a Dionex UltiMate 3000 isocratic pump and a RefractoMax 521 refractive index detector, was used to measure the molecular weight. The measurements were performed at 25 °C and a flow rate of 1 $mL{\cdot}min^{-1}$. The

Table 1
Amount of reagents used.

Samples	IPDI [g (mmol)]	PCL [g (mmol)]	DMPA [g (mmol)]	TEOA [g (mmol)]	HEMA [g (mmol)]
PU_PCL/TEOA_100/0	6.22 (28.00)	32.00 (16.00)	1.07 (8.00)	–	1.07 (8.00)
PU_PCL/TEOA_75/25		24.00 (12.00)		0.60 (4.00)	
PU_PCL/TEOA_50/50		16.00 (8.00)		1.19 (8.00)	
PU_PCL/TEOA_25/75		8.00 (4.00)		1.80 (12.00)	

samples were prepared drying the final dispersions in a dark place for 1 week at room temperature. 10–20 mg of the dried sample were dissolved in 1 mL of tetrahydrofuran (THF) and the solutions were filtered before injection. The calibration was made with polystyrene standards of a range of 162–3,150,000 g·mol^{-1}.

The gel content (GC) of the synthesised samples before and after curing was determined by Soxhlet extraction in THF and DMF. The samples were dried for 24 h at 60 °C before and after extraction. The extraction process proceeded in boiling THF and DMF for 24 h. The final data obtained were an average of three.

A Phoenix 300 goniometer from Surface Electro Optics with an image processing system from Data Physics Instruments GmbH was employed to measure the static contact angle (CA). Measurements were performed with distilled water droplets of about 15–20 μL, after a contact period of 30 s, and registered CA was an average value of at least eight readings.

Water vapour transmission rate (WVTR) was measured employing a polytetrafluoroethylene gravimetric permeation cell following ASTM E96-95. The partially filled cell was sealed with the membrane to be analysed. Weight loss due to the permeation through the membrane was measured with a Sartorius BP210D balance. The measurements were performed at room temperature (25 °C) and relative humidity of about 55.5 % RH. Samples were prepared following the same procedure employed in the Soxhlet extraction and the results obtained were an average of three measurements. The film thickness was measured by a Duo-Check ST-10 apparatus (Neurtek Instruments).

The obtained data for gel content, and water vapour transmission rate were analysed by variance analysis (ANOVA) with Tukey's multiple comparison tests at $p < 0.05$ to identify the differences between groups.

Dynamic-mechanical analysis (DMA) was performed on an Eplexor 100N (Gabo Qualimeter) at 1 Hz, in a single cantilever bending mode, with an elastic deformation of 0.5 % and a dynamic deformation of 0.2 % from −80 °C to 150 °C at a heating rate of 2 °C·min^{-1}. The samples employed were 5 × 10 × 3 mm^3 rectangular stripes. The samples were prepared as for WVTR measurements. The storage modulus (E′), loss modulus (E″), and their ratio (tan δ = E′/E″), known as loss factor or damping, were quantified.

3. Results and discussions

3.1. Synthesis and characterization of the polyurethane prepolymer

The urethane group formation by reaction between the isocyanate and different alcohols was monitored by FTIR. For this purpose, samples were removed from the reactor at different times and placed on the ATR crystal. The spectra were recorded after acetone evaporation (5 min). Fig. 1 shows the spectra for samples PU_PCL/TEOA_50/50. As the reaction progressed, bands related to the isocyanate and alcohol groups decreased and those concerning the urethane groups increased. Hence, the isocyanate υ N═C═O band at 2260 cm^{-1} decreased with time, and amide I (υ C═O at 1715 cm^{-1}) and amide II (δ —NH at 1530 cm^{-1}) absorption bands of the urethane increased [13,25]. In the OH stretching vibration region (3600–3200 cm^{-1}) bands related alcohol groups decreased, but they were overlapped with the generated NH stretching vibration. It is worth mentioning that PCL carbonyl stretching (υ C═O at 1735 cm^{-1}) overlapped with the urethane amide I carbonyl.

Accordingly, for all the cases the overall reaction conversion was monitored by analysing the isocyanate characteristic band (2260 cm^{-1}) reduction and normalizing the value with methyl and methylene group stretching vibration bands between 2800 cm^{-1} and 3000 cm^{-1} [26]. The final conversion values obtained in the different reactions are summarised in Table 2. As expected, almost total conversion was registered in all the reactions.

The molecular weight of the polymers obtained in the different reactions are summarised in Table 2. The slight increase of $\overline{M_w}$ from PU_PCL/TEOA_100/0 to PU_PCL/TEOA_75/25 was related to the trifunctional nature of TEOA that allowed the crosslinking of the polymer. Therefore, although TEOA was considered as difunctional when calculating the stoichiometry, partial crosslinking happened. However, for the higher TEOA percentages the molecular weight was not measured because the samples were not soluble in THF. This fact was related in addition to the previously mentioned partial crosslinking, to the ionic

Table 2
Polyurethane conversion, molecular weight data, and dispersions properties.

Samples	Conversion [%]	$\overline{M_n}$ [g·mol^{-1}]	$\overline{M_w}$ [g·mol^{-1}]	Đ	IEP
PU_PCL/TEOA_100/0	97	22,537	47,845	2.1	4.5
PU_PCL/TEOA_75/25	97	23,775	56,140	2.4	4.8
PU_PCL/TEOA_50/50	100	/	/	/	4.1
PU_PCL/TEOA_25/75	100	/	/	/	5.0

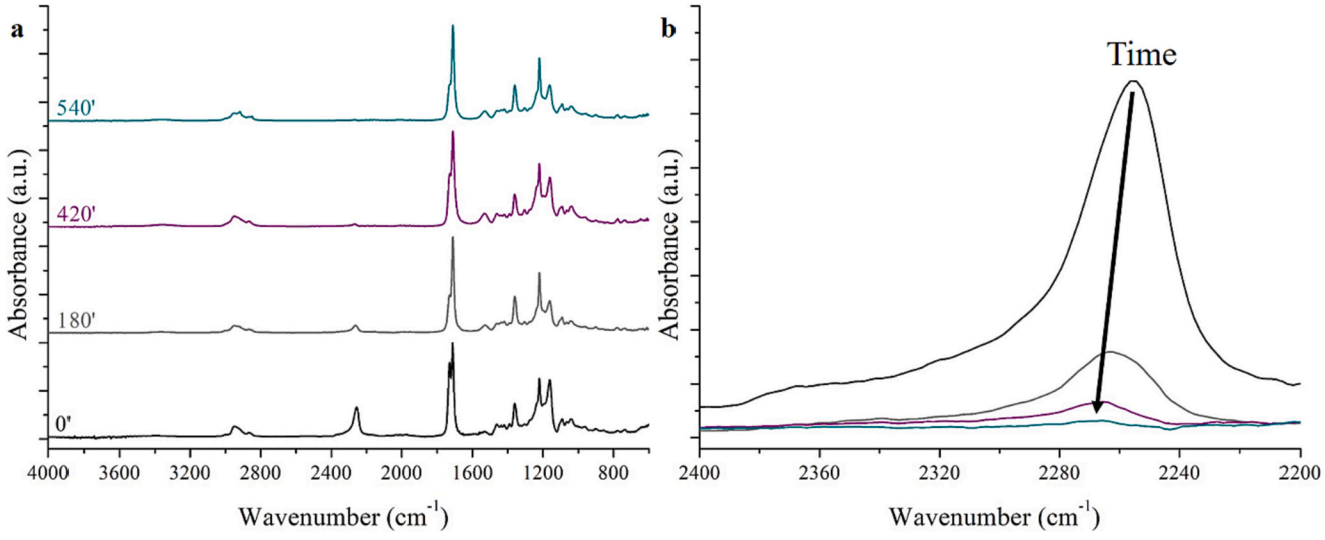

Fig. 1. a) FTIR and b) scale-expanded spectra between 2400 and 2200 cm^{-1} of PU_PCL/TEOA_50/50 samples at different polyurethane polymerisation reaction stages.

interaction between the acid groups of the DMPA and the tertiary nitrogen of TEOA that prevented the solution in THF. This effect is also analysed in the section devoted to gel content results.

After the polyurethane synthesis, water was added to produce the phase inversion. Some experiments were performed without neutralizing the DMPA acid groups with triethylamine (TEA) but no stable dispersions were obtained. This effect was attributed to the ionic acid/base interaction between DMPA and TEOA. Therefore, the incorporation of TEA was necessary in order to avoid the polymer/polymer interaction and all the dispersions were obtained after the incorporation of TEA. It can be argued that instead of deprotonating the acid groups, stable dispersions would have been obtained protonating TEOA. However, as anionic emulsifiers tend to provide better application properties the first option was chosen.

The IEP is known as the pH value at which the charges in the chain are zero [27]. The values in the different dispersions were measured, and the results are shown in Table 2. As observed, regardless of sample composition, values around 4–5 were obtained. These values were related to the protonation at low pH of the carboxylate groups of the DMPA [28]. When the pH values were lower than the IEP, the particles aggregated and precipitation occurred in the PU_PCL/TEOA_100/0 sample. The other samples presented higher stability.

The particle size of all the dispersions was measured in a pH range from 12 to 3. The results are shown in Fig. 2. As observed, at basic pH the particle size of all the dispersions was between 100 and 200 nm. Moreover, the particle size distribution increased with the TEOA addition. According to literature, when the polyol length is higher, more flexible chains are obtained, which allows the fragmentation of the prepolymer to primary particles of the dispersed phase to smaller and more homogeneous particles [29]. In the sample PU_PCL/TEOA_25/75, the particle size showed two different populations. This fact was related to the high hydroxyl excess employed in the stoichiometry of this reaction since TEOA was considered as difunctional for the reagent amount calculation. Therefore, the formulation presumably contained free TEOA and was non-homogeneous. In all the formulations, when the pH was reduced the particle size increased because of the protonation of the acid groups of the DMPA.

The particle size as a function of the pH of the samples excluding the previously mentioned PU_PCL/TEOA_25/75 sample is shown in Fig. 3. As observed, the particle size remained similar until pH 6 (close to the isoelectric point) where a huge increase of the value was observed for the sample without TEOA that presented a particle size close to 700 nm at low pH. However, the increase of the particle size at low pH of the

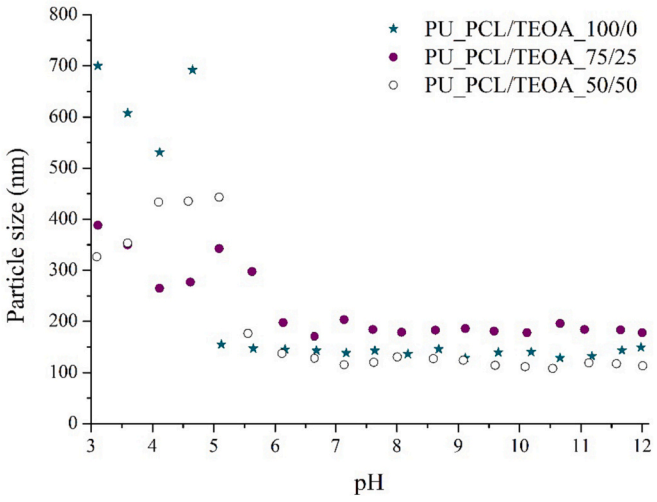

Fig. 3. The particle size of the different samples with pH values.

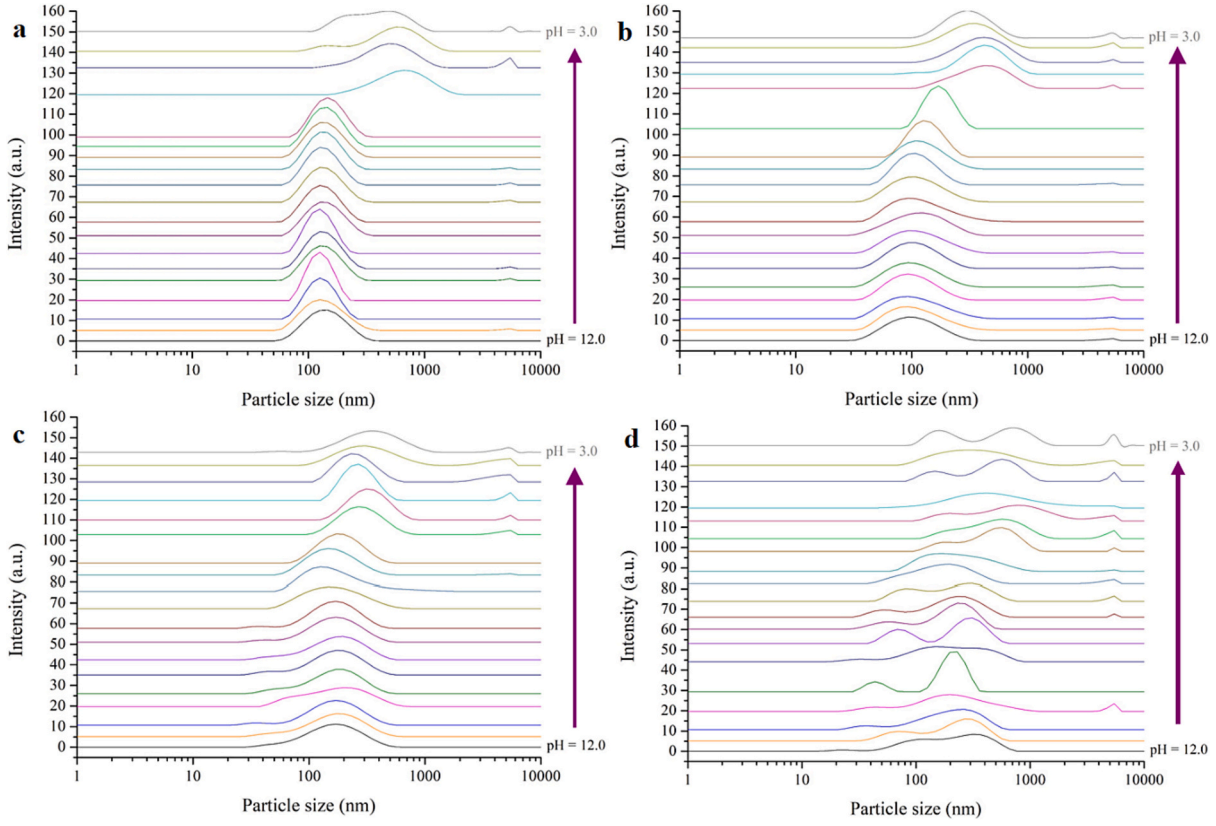

Fig. 2. Particle size measurements at different pH values for samples a) PU_PCL/TEOA_100/0, b) PU_PCL/TEOA_75/25, c) PU_PCL/TEOA_50/50, and d) PU_PCL/TEOA_25/75.

TEOA containing samples was lower. This effect was related to the protonation of the tertiary amine at low pH. Consequently, in an acid medium, the stabilising effect of DMPA was cancelled, but the protonation of the TEOA gave rise to cationic stabilisation. However, the stabilisation was not as effective as the anionic one since the particle size increased at low pH. Accordingly, the results showed that the samples containing TEOA in addition to DMPA were amphoteric, and more stable dispersions were obtained after the IEP. Consequently, they can be employed in a wider range of pH. However, for highest TEOA concentration, the change in the NCO/OH ratio provoked the formation of non-homogeneous dispersion that presented low stability towards pH changes.

3.2. Synthesis and characterization of the final polyurethane

Films were obtained after the addition of the photo-initiator and water removal in the dark. Afterwards, samples were cured, and FTIR spectra were recorded before and after UV irradiation (Fig. S1). The decrease of the =C—H double bond out-of-plane bending band at 810 cm^{-1} [30,31] showed that UV irradiation provoked the polymerisation of the acrylic double bond. However, the area of this band was too low to follow the reaction as reported in previous works [30]. Accordingly, the curing reaction was followed by photo-DSC. Fig. 4a shows the polymerisation rate for the sample PU_PCL/TEOA_100/0 containing different amounts of photo-initiator. As observed, some final values were higher than 100 % because of the errors involved in the calculation. The results showed that the polymerisation rate increased and it reached its maximum after some seconds and afterward decreased due to the immobilisation caused by the curing [30]. Moreover, as expected, the photo-initiator amount caused an increase in the polymerisation rate. In addition, it should be noted that the increment in the photo-initiator amount from 0.5 to 1 wt% increased the final polymerisation conversion (Fig. 4b). This could be explained by the increment of free radical formation. However, similar final conversion values were obtained for a photo-initiator amount of 1 and 1.5 wt%.

The effect of TEOA in the photo-polymerisation process was analysed for samples with a photo-initiator content of 1.5 wt%, and the polymerisation rate and conversion are shown in Fig. 5. It can be highlighted that the incorporation of TEOA increased the polymerisation rate. This fact was related to the lower PCL content of the samples when the TEOA concentration was increased. Considering that the photo-polymerisation happened at room temperature, the PCL crystals could reduce the radical diffusion decreasing the polymerisation rate. However, the samples PU_PCL/TEOA_75/25 and PU_PCL/TEOA_50/50 did to reach total conversion (Fig. 5b). This effect was caused by the diffusional limitations in the polymerisation reaction due the acid/base interaction of the samples [32]. However, for the sample PU_PCL/TEOA_25/75_1.5 % higher conversion was obtained. This was explained by the high hydroxyl excess employed in the polymerisation of the sample that increased the chain mobility.

The gel contents for the samples in both THF and DMF are shown in Table 3. According to the data obtained for THF, as expected, the gel content increased when the radical reaction took place. However, no difference was observed concerning the initiator amount, unlike the previously concluded in the photo-DSC analysis. The authors attribute this to the fact that the UV reaction is limited by the exposed surface when large scales are employed. Since in real application, as coatings, the thickness is low it was considered that this effect would not happen.

Moreover, the incorporation of TEOA caused the increment of the gel content in THF to such an extent that before curing a value of 75 % was obtained for the sample PU_PCL/TEOA_50/50. As TEOA is a trifunctional compound cross-linked chains could be obtained. Additionally, it could be argued that the acid groups of DMPA and the tertiary amine groups of TEOA were able to create ionic bonds when dried [33]. To corroborate this, the extractions were repeated in a more polar solvent able to break the ionic interactions (DMF). The results showed that when DMF was employed, before the acrylic polymerisation, the gel content of samples PU_PCL/TEOA_50/50 and PU_PCL/TEOA_25/75 decreased significantly concluding that TEOA was able to create ionic bonds, which were destroyed when dissolving in DMF. This effect was especially relevant in the sample PU_PCL/TEOA_50/50 since it presented an equimolecular concentration of acid and tertiary amine groups that favoured the ionic interaction. Accordingly, the highest gel content in both solvents were obtained for the 1/1 acid/amine molar ratio. The gel content of the sample containing the highest TEOA concentration (PU_PCL/TEOA_25/75) when extracted with DMF was very low. This result demonstrated that this sample was not covalently cross-linked and that the insolubility in THF was because of the ionic interaction between the amine and acid groups. This was related again to the high hydroxyl excess of this sample that prevents correct cross-linking. FTIR spectra of samples before and after DMF extraction were recorded but no differences were observed (see Fig. S2).

TGA and DTGA measurements of all the samples before curing are collected in Fig. 6 and the UV-cured samples with 1 wt% of photo-initiator in Fig. 7. In both cases, the sample PU_PCL/TEOA_25/75 showed a reduced thermal stability since the weight loss process started at lower temperature. This result was related to the excess of hydroxyl groups employed in the synthesis of this sample that gave rise to the

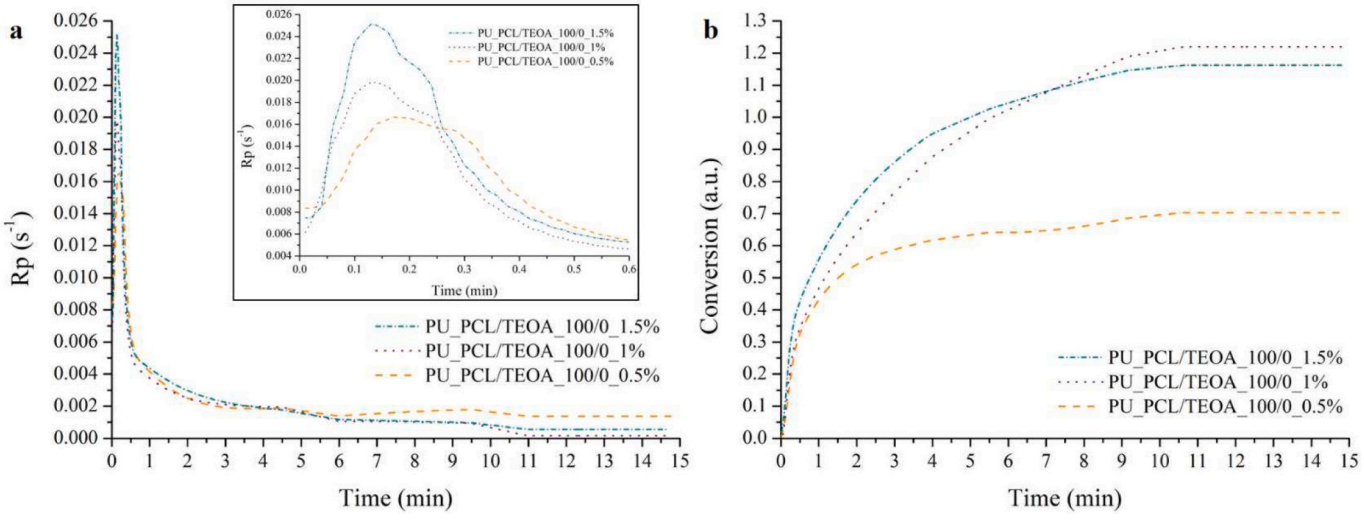

Fig. 4. a) Polymerisation rate and b) conversion of UV curing obtained from photo-DSC of sample PU_PCL/TEOA_100/0 with different initiator concentration.

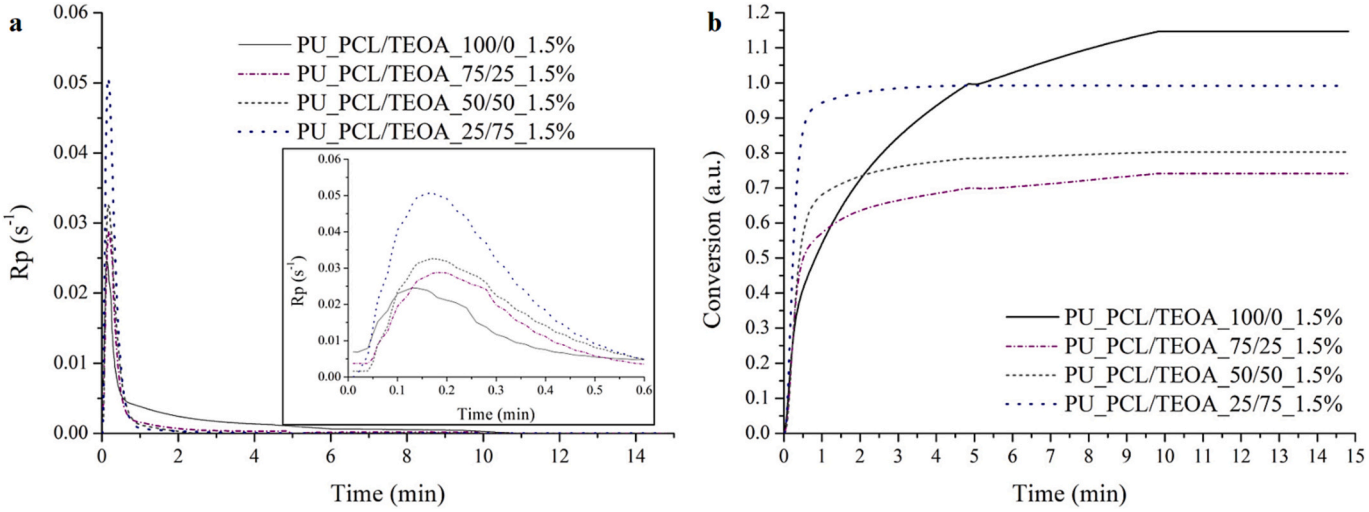

Fig. 5. a) Polymerisation rate and b) conversion of UV curing obtained from photo-DSC of samples with 1.5 wt% initiator with different TEOA concentration.

Table 3
Properties of the obtained films.

Samples	Initiator [wt%]	GC THF [%]	GC DMF [%]	CA [°]
PU_PCL/TEOA_100/0	0	0	0	80 ± 5
	0.5	28 ± 3	21 ± 5	82 ± 4
	1	27 ± 2	–	82 ± 3
	1.5	29 ± 1	–	81 ± 4
PU_PCL/TEOA_75/25	0	0	0	83 ± 3
	0.5	49 ± 1	46 ± 10	81 ± 4
	1	52 ± 7	–	84 ± 3
	1.5	53 ± 2	–	83 ± 4
PU_PCL/TEOA_50/50	0	75 ± 2	47 ± 7	80 ± 1
	0.5	84 ± 7	76 ± 10	81 ± 3
	1	81 ± 2	–	83 ± 1
	1.5	76 ± 2	–	83 ± 1
PU_PCL/TEOA_25/75	0	23 ± 3	2 ± 1	86 ± 4
	0.5	59 ± 1	9 ± 6	86 ± 3
	1	58 ± 2	–	90 ± 5
	1.5	55 ± 2	–	91 ± 4

formation of low molecular weight species that presented lower thermal stability. Excluding this sample all the films showed a similar behaviour. Thus, the films were stable until 250 °C where according to literature polyurethanes start to degrade from the hard segment [34,35]. Moreover, no significant differences were observed in the initial thermal stability of the samples and accordingly it was stated that the curing process did not increase the thermal stability of the samples [35–37]. However, the incorporation of TEOA broadened the curve (as observed clearly in the DTGA curves), increasing the thermal stability at high temperatures.

Fig. S3 shows the conventional DSC run for samples PU_PCL/TEOA_100/0 with different initiator amounts and the data for all the samples are summarised in Table 4. In the first run, an endotherm peak was appreciable at about 45 °C (T_m), which indicates that the PCL chains were able to fold and form crystalline structures [38,39]. In the second heating run cold crystallisation was appreciable, so the data obtained were collected from the first run [40,41]. Based on the first run, the polymer crystallinity (X_c) degree was calculated, which decreased with the photo-initiator concentration. The decrease in the crystallinity was related to the cross-linking generated by the acrylic double bonds since the cross-linking restricts the chain mobility and prevents the lamellae arrangement [42]. Similarly, a slight decrease was appreciable in the PCL glass-transition temperature (T_g) with the photo-initiator concentration. This decrease could be explained by the decrease in the PCL crystallinity, which restricted chain mobility. Therefore, the higher photo-initiator concentration caused a decrease in the PCL crystallinity and a decrease in the T_g. Noteworthy, there was not a clear hard-segment glass transition temperature, as stated by other authors in the literature [43].

When TEOA was incorporated a reduction of the crystallinity degree and melting temperature of the PCL happened (see Fig. S4 and results in

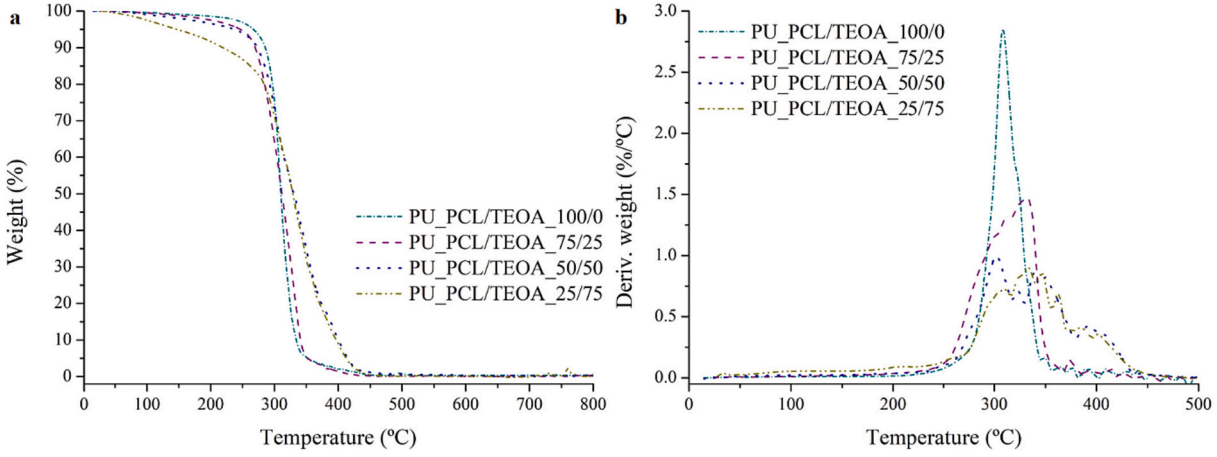

Fig. 6. a) TGA and b) DTG curves of the different films.

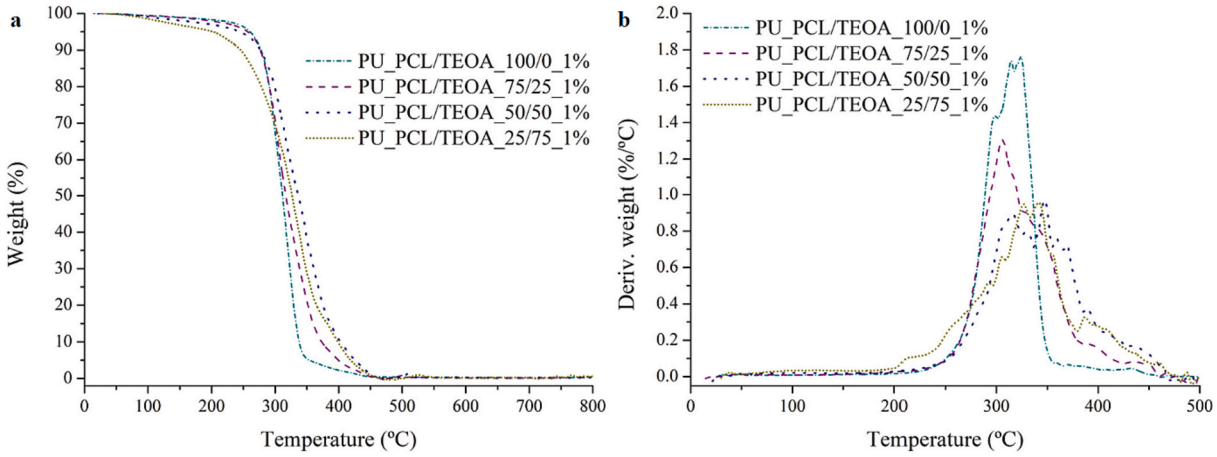

Fig. 7. a) TGA and b) DTG curves of the different films with 1.0 wt% initiator.

Table 4
Data obtained from DSC results.

Samples	Initiator [wt %]	T_m [°C]	ΔH [J·g^{-1}]	X_c [% PCL]	T_g [°C]
PU_PCL/ TEOA_100/0	0	46	43	41	−46
	0.5	46	36	34	−46
	1	46	38	37	−48
	1.5	46	34	32	−48
PU_PCL/ TEOA_75/25	0	39	26	27	−47
	0.5	44	27	29	−48
	1	44	25	27	−50
	1.5	45	13	13	−53
PU_PCL/ TEOA_50/50	0	38	17	21	−53
	0.5	43	14	17	−51
	1	43	14	17	−53
	1.5	43	14	17	−52
PU_PCL/ TEOA_25/75	0	41	7	12	−56
	0.5	46	1	2	−59
	1	48	3	5	−54
	1.5	47	3	5	−58

Table 4). As the different formulations were obtained replacing the PCL by TEOA the samples containing higher TEOA concentration presented lower PCL content. As a consequence, the PCL segments were more isolated in a more rigid medium preventing the crystallisation. The T_g values were also reduced with the TEOA concentration because the decrease in the PCL crystallinity, which restricted chain mobility.

The DMA results for the samples before and after curing are shown in Figs. 8 and 9, respectively. According to the loss factor results, T_g values similar to those obtained by DSC were obtained. In addition, before curing the glassy state storage modulus increased with the TEOA content of the samples. This effect was related to a reduction of the chain flexibility when replacing PCL by a short alcohol [44]. Sample PU_PCL/TEOA_25/75 showed a different behaviour probably related to the high hydroxyl excess employed in this formulation. Additionally, except for this sample, the rubbery plateau showed higher values with the incorporation of TEOA, due to either cross-linking caused by the trifuntionality or ionic forces. All the samples showed a huge decrease of the storage modulus close to the PCL melting temperature. As expected, the incorporation of TEOA shifted the decrease to lower temperatures since it reduced the PCL crystallisation degree (as shown by the DSC results) [44]. After curing, the sample without TEOA and the sample containing the highest TEOA concentration (PU_PCL/TEOA_25/75) showed higher storage modulus values than the others. This result was related to the acrylic conversion studied by photo-DSC that was higher in these two samples.

Therefore, a general tendency of the storage modulus when increasing the TEOA content could not be established since the amphoteric character affected the acrylic conversion and the PCL crystallinity degree. Thus, it was not possible to separate the effect of the acid/base ionic interaction from the changes originated in the covalent crosslinking degree of the samples.

The contact angle of the samples was measured, and the results are shown in Table 3. As observed, all the samples presented contact angles close to 80°. The water vapour transmission rate (WVTR) data are shown

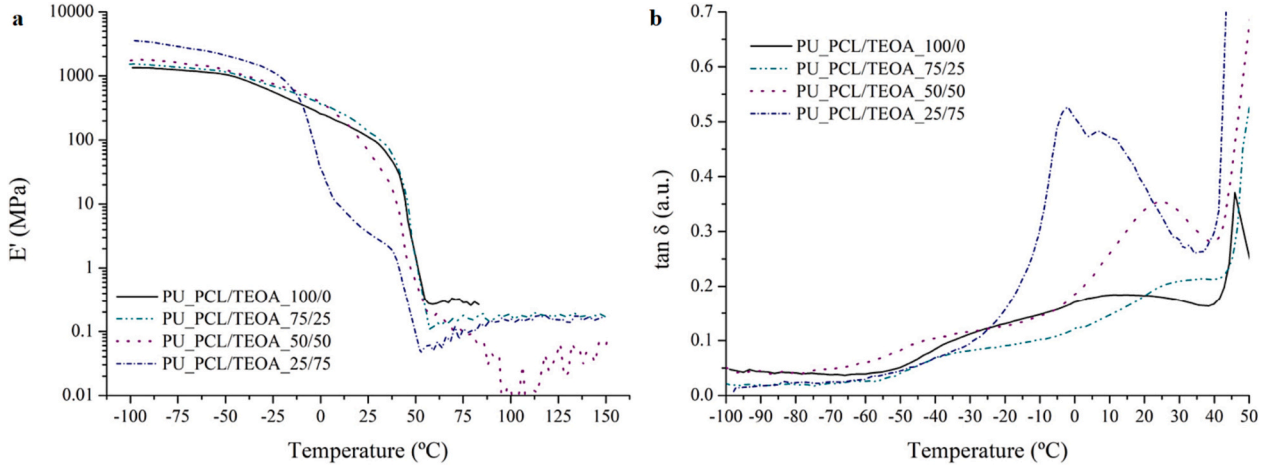

Fig. 8. a) Storage modulus and b) loss factor data.

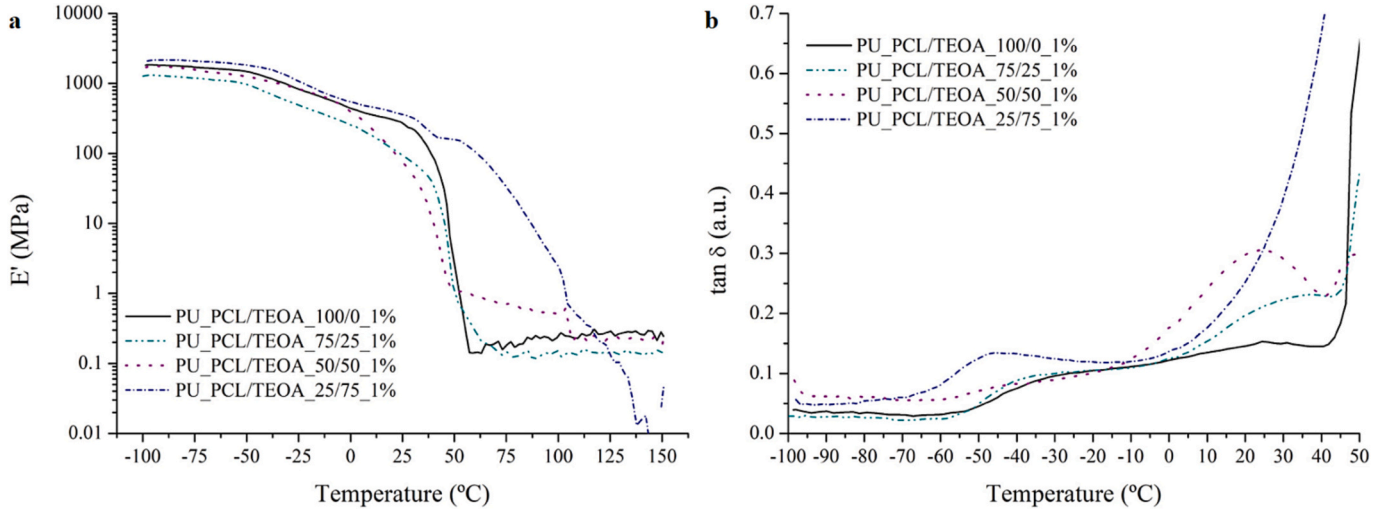

Fig. 9. a) Storage modulus and b) loss factor data for cured samples containing 1 wt% initiator.

in Fig. 10. As observed, WVTR values decreased with the incorporation of TEOA into the chain until sample PU_PCL/TEOA_50/50. According to the literature, this behaviour was related to the generation of a rigid ionic complexed network that acts as a physical obstacle against water penetration [45]. Sample PU_PCL/TEOA_50/50 presented the lowest WVTR since it was obtained using the equimolar ratio between the acid and amine groups. Sample PU_PCL/TEOA_25/75, containing the highest TEOA concentration showed higher WVTR values. In order this behaviour to be explained different factors should be borne in mind. On the one hand in this sample, the DMPA/TEOA mol ratio was 1/1.5 and therefore the excess of tertiary amine groups could favour the water solubility. On the other hand, according to gel content measurement, this sample presented low covalent cross-linking. This could provoke an increase in the water diffusivity that reduced the tortuous path of the penetrant. Both factors provoked the increase in the WVTR in this sample that presented the penetrant. Both factors provoked the increase in the WVTR in this sample that presented the highest values.

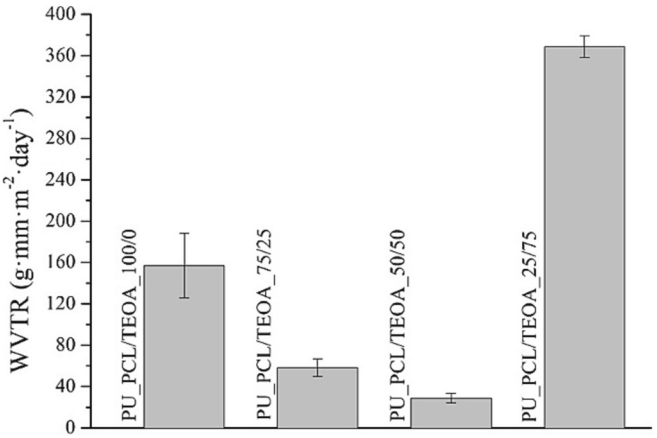

Fig. 10. Water vapour transmission rate data for cured samples containing 1.5 wt% initiator at room temperature.

4. Conclusions

In this study, waterborne UV-curable polyurethane dispersions with amphoteric properties were successfully synthesised by incorporating triethanolamine (TEOA) in addition to conventional anionic internal surfactant. The dispersions showed excellent stability against pH variations, attributed to the amphoteric nature imparted by TEOA. Therefore, the colloidal stability of the dispersions was maintained at low pH. The best properties were obtained for the samples containing 1/1 amine/acid molar ratio. Thus, while the anionic dispersions coagulated at low pH values the 1/1 amphoteric dispersion showed high stability to pH changes. After curing this sample with UV irradiation, the gel content of the film was higher and the water vapour transmission rate was lower than that of the conventional polyurethane because of the strong acid/base interaction. All these results demonstrate the potential of amphoteric WPUs for applications requiring stability over a broad pH spectrum, and can be of great interest for the development of environmentally friendly coatings and adhesives. Further exploration of specific applications and optimisation of formulation parameters could improve the performance and versatility of these amphoteric UV-curable WPUs.

CRediT authorship contribution statement

M. Puyadena: Writing – original draft, Investigation. **E. Pajares:** Investigation. **L. Martin:** Investigation, Data curation. **A. Barrio:** Conceptualization. **A. González:** Writing – original draft, Conceptualization. **L. Irusta:** Writing – original draft, Conceptualization.

Declaration of competing interest

The authors declare that they have no known competing financial interests or personal relationships that could have appeared to influence the work reported in this paper.

Data availability

Data will be made available on request.

Acknowledgments

The University of the Basque Country (UPV/EHU) predoctoral grant of M. Puyadena and the funding by the Basque Government through grant IT1667-22 are gratefully acknowledged. Technical and human support provided by SGIker is also sincerely acknowledged (UPV/EHU/ERDF, EU).

Appendix A. Supplementary data

Supplementary data to this article can be found online at https://doi.

org/10.1016/j.porgcoat.2024.108229.

References

[1] K.-L. Noble, Waterborne polyurethanes, Prog. Org. Coatings. 32 (1997) 131–136, https://doi.org/10.1016/S0300-9440(97)00071-4.

[2] B.K. Kim, Aqueous polyurethane dispersions, Colloid Polym. Sci. 274 (1996) 599–611, https://doi.org/10.1007/BF00653056.

[3] R.K. Gupta, A.K. Mishra, Eco-Friendly Waterborne Polyurethanes: Synthesis, Properties, and Applications, 1st ed, Taylor & Francis, 2022, https://doi.org/10.1201/9781003173526.

[4] D.K. Chattopadhyay, K.V.S.N. Raju, Structural engineering of polyurethane coatings for high performance applications, Prog. Polym. Sci. 32 (2007) 352–418, https://doi.org/10.1016/j.progpolymsci.2006.05.003.

[5] M. Barrère, K. Landfester, High molecular weight polyurethane and polymer hybrid particles in aqueous miniemulsion, Macromolecules 36 (2003) 5119–5125, https://doi.org/10.1021/ma025981+.

[6] M.A. Pérez-Limiñana, F. Arán-Aís, A.M. Torró-Palau, A.C. Orgilés-Barceló, J. M. Martín-Martínez, Characterization of waterborne polyurethane adhesives containing different amounts of ionic groups, Int. J. Adhes. Adhes. 25 (2005) 507–517, https://doi.org/10.1016/j.ijadhadh.2005.02.002.

[7] H. Sardon, L. Irusta, M.J. Fernández-Berridi, J. Luna, M. Lansalot, E. Bourgeat-Lami, Waterborne polyurethane dispersions obtained by the acetone process: a study of colloidal features, J. Appl. Polym. Sci. 120 (2011) 2054–2062, https://doi.org/10.1002/app.33308.

[8] A.K. Nanda, D.A. Wicks, The influence of the ionic concentration, concentration of the polymer, degree of neutralization and chain extension on aqueous polyurethane dispersions prepared by the acetone process, Polymer (Guildf.) 47 (2006) 1805–1811, https://doi.org/10.1016/j.polymer.2006.01.074.

[9] B.K. Kim, Y.M. Lee, Aqueous dispersion of polyurethanes containing ionic and nonionic hydrophilic segments, J. Appl. Polym. Sci. 54 (1994) 1809–1815, https://doi.org/10.1002/app.1994.070541204.

[10] F. Tabatabaee, M. Khorasani, M. Ebrahimi, A. González, L. Irusta, H. Sardon, Synthesis and comprehensive study on industrially relevant flame retardant waterborne polyurethanes based on phosphorus chemistry, Prog. Org. Coatings 131 (2019) 397–406, https://doi.org/10.1016/j.porgcoat.2019.02.042.

[11] M. Cobos, E. Pagalday, M. Puyadena, X. Cabido, L. Martin, A. Múgica, L. Irusta, A. Gonz, Waterborne hybrid polyurethane coatings containing casein as sustainable green flame retardant through different synthesis approaches, Prog. Org. Coatings 174 (2023) 107278, https://doi.org/10.1016/j.porgcoat.2022.107278.

[12] H. Xu, F. Qiu, Y. Wang, W. Wu, D. Yang, Q. Guo, Progress in organic coatings UV-curable waterborne polyurethane-acrylate: preparation, characterization and properties, Prog. Org. Coatings 73 (2012) 47–53, https://doi.org/10.1016/j.porgcoat.2011.08.019.

[13] M. Puyadena, I. Etxeberria, L. Martin, A. Mugica, A. Agirre, M. Cobos, A. Gonzalez, A. Barrio, L. Irusta, Polyurethane/acrylic hybrid dispersions containing phosphorus reactive flame retardants as transparent coatings for wood, Prog. Org. Coatings 170 (2022) 107005, https://doi.org/10.1016/j.porgcoat.2022.107005.

[14] P. Musto, G. Ragosta, G. Scarinzi, L. Mascia, Properties of amphoteric polyurethane waterborne dispersions. I. Dependence on pH value in salt-free media, J. Polym. Sci. Part B Polym. Phys. 40 (2002) 972–979, https://doi.org/10.1002/polb.10153.

[15] A. Dong, G. Hou, D. Sun, Properties of amphoteric polyurethane waterborne dispersions II. Macromolecular self-assembly behavior, J. Colloid Interface Sci. 266 (2003) 276–281, https://doi.org/10.1016/S0021-9797(03)00580-0.

[16] C. Wang, C. Ma, C. Mu, W. Lin, A novel approach for synthesis of zwitterionic polyurethane coating with protein resistance, Langmuir 30 (2014) 12860–12867, https://doi.org/10.1021/la503426e.

[17] C. Ma, H. Zhou, B. Wu, G. Zhang, Preparation of polyurethane with zwitterionic side chains and their protein resistance, ACS Appl. Mater. Interfaces 3 (2011) 455–461, https://doi.org/10.1021/am101039q.

[18] S. Chen, F. Mo, Y. Yang, F.J. Stadler, S. Chen, H. Yang, Z. Ge, Development of zwitterionic polyurethanes with multi-shape memory effects and self-healing properties, J. Mater. Chem. A 3 (2015) 2924–2933, https://doi.org/10.1039/c4ta06304j.

[19] X. Li, E. Zhang, J. Shi, X. Xiong, J. Lin, Q. Zhang, X. Cui, L. Tan, K. Wu, Waterborne polyurethane enhanced, adhesive, and ionic conductive hydrogel for multifunctional sensors, Macromol. Rapid Commun. 42 (2021) 1–10, https://doi.org/10.1002/marc.202100457.

[20] B.B. Champati, B.M. Padhiari, A. Ray, S. Jena, A. Sahoo, S. Mohanty, J. Patnaik, P. K. Naik, P.C. Panda, S. Nayak, Implementation of multilayer perceptron (MLP) and radial basis function (RBF) neural networks for predicting Shatavarin IV content in Asparagus racemosus accessions, Ind. Crop. Prod. 191 (2023) 115968, https://doi.org/10.1016/j.indcrop.2022.115968.

[21] Z. Ren, L. Liu, H. Wang, Y. Fu, L. Jiang, B. Ren, Novel amphoteric polyurethane dispersions with postpolymerization crosslinking function derived from hydroxylated tung oil: synthesis and properties, RSC Adv. 5 (2015) 27717–27721, https://doi.org/10.1039/c5ra03115j.

[22] S. Boufi, M.N. Belgacem, J. Quillerou, A. Gandini, Urethanes and polyurethanes bearing furan moieties. 4. Synthesis, kinetics, and characterization of linear polymers sami, Macromolecules 26 (1993) 6706–6717, https://doi.org/10.1021/ma00077a003.

[23] H.D. Hwang, C.H. Park, J.I. Moon, H.J. Kim, T. Masubuchi, UV-curing behavior and physical properties of waterborne UV-curable polycarbonate-based polyurethane dispersion, Prog. Org. Coatings 72 (2011) 663–675, https://doi.org/10.1016/j.porgcoat.2011.07.009.

[24] H. Kweona, M.K. Yoob, I. KyuParkb, T.H. Kimb, H.C. Leec, H.-S. Leec, J.-S. Ohc, T. Akaiked, Chong-Su Chob, A novel degradable polycarbonate networks for tissue engineering, Biomaterials 24 (2003) 801–808, https://doi.org/10.1016/S0142-9612(02)00370-8.

[25] A. Santamaria-Echart, A. Arbelaiz, A. Saralegi, B. Fernández-d'Arlas, A. Eceiza, M. A. Corcuera, Relationship between reagents molar ratio and dispersion stability and film properties of waterborne polyurethanes, Colloids Surf. A Physicochem. Eng. Asp. 482 (2015) 554–561, https://doi.org/10.1016/j.colsurfa.2015.07.012.

[26] C. Chai, J. Hou, X. Yang, Z. Ge, M. Huang, G. Li, Two-component waterborne polyurethane: curing process study using dynamic in situ IR spectroscopy, Polym. Test. 69 (2018) 259–265, https://doi.org/10.1016/j.polymertesting.2018.05.021.

[27] A. Dong, G. Hou, M. Feng, A. Li, Properties of amphoteric polyurethane waterborne dispersions. III. Isoelectric points and precipitation, J. Polym. Sci. Part B Polym. Phys. 40 (2002) 2440–2448, https://doi.org/10.1002/polb.10303.

[28] Y. Li, B.A.J. Noordover, R.A.T.M. Van Benthem, C.E. Koning, Chain extension of dimer fatty acid- and sugar-based polyurethanes in aqueous dispersions, Eur. Polym. J. 52 (2014) 12–22, https://doi.org/10.1016/j.eurpolymj.2013.12.007.

[29] A.C. Ospina, V.H. Orozco, L.F. Giraldo, M. Fuensanta, J.M. Martín-Martínez, N. Mateo-Oliveras, Study of waterborne polyurethane materials under aging treatments. Effect of the soft segment length, Prog. Org. Coatings 138 (2020), https://doi.org/10.1016/j.porgcoat.2019.105357.

[30] O. Llorente, M.J. Fernández-Berridi, A. González, L. Irusta, Study of the crosslinking process of waterborne UV curable polyurethane acrylates, Prog. Org. Coatings 99 (2016) 437–442, https://doi.org/10.1016/j.porgcoat.2016.06.020.

[31] D. Kunwong, N. Sumanochitraporn, S. Kaewpirom, Curing behavior of a UV-curable coating based on urethane acrylate oligomer: the influence of reactive monomers, Songklanakarin, J. Sci. Technol. 33 (2011) 201–207.

[32] T.J. Tulig, M. Tirrell, On the onset of the Trommsdorff effect, Macromolecules 15 (1982) 459–463, https://doi.org/10.1021/ma00230a050.

[33] M. Argaiz, F. Ruipérez, M. Aguirre, R. Tomovska, Ionic inter-particle complexation effect on the performance of waterborne coatings, Polymers (Basel) 13 (2021) 1–18, https://doi.org/10.3390/polym13183098.

[34] J.M. Cervantes-Uc, J.I.M. Espinosa, J.V. Cauich-Rodríguez, A. Ávila-Ortega, H. Vázquez-Torres, A. Marcos-Fernández, J.S. Román, TGA/FTIR studies of segmented aliphatic polyurethanes and their nanocomposites prepared with commercial montmorillonites, Polym. Degrad. Stab. 94 (2009) 1666–1677, https://doi.org/10.1016/j.polymdegradstab. 2009.06.022.

[35] Z. Niu, F. Bian, Synthesis and characterization of multiple cross-linking UV-curable waterborne polyurethane dispersions, Iran, Polym. J. (English Ed.) 21 (2012) 221–228, https://doi.org/10.1007/s13726-012-0021-6.

[36] M.M. Ghobashy, Z.I. Abdeen, Radiation crosslinking of polyurethanes: characterization by FTIR, TGA, SEM, XRD, and Raman spectroscopy, J. Polym. 2016 (2016) 1–9, https://doi.org/10.1155/2016/9802514 Research.

[37] J. Brzeska, A. Tercjak, W. Sikorska, M. Kowalczuk, M. Rutkowska, Predicted studies of branched and cross-linked polyurethanes based on polyhydroxybutyrate with polycaprolactone triol in soft segments, Polymers (Basel) 12 (2020), https://doi.org/10.3390/POLYM12051068.

[38] X. Feng, G. Wang, K. Neumann, W. Yao, L. Ding, S. Li, Y. Sheng, Y. Jiang, M. Bradley, R. Zhang, Synthesis and characterization of biodegradable poly(ether-ester) urethane acrylates for controlled drug release, Mater. Sci. Eng. C 74 (2017) 270–278, https://doi.org/10.1016/j.msec.2016.12.009.

[39] T. Zhang, W. Wu, X. Wang, Y. Mu, Effect of average functionality on properties of UV-curable waterborne polyurethane-acrylate, Prog. Org. Coatings 68 (2010) 201–207, https://doi.org/10.1016/j.porgcoat.2010.02.004.

[40] H.A. Ranjbar, M. Nourany, M. Mollavali, F. Noormohammadi, S. Jafari, Stimuli-responsive polyurethane bionanocomposites of poly(ethylene glycol)/poly (ε-caprolactone) and [poly(ε-caprolactone)-grafted-] cellulose nanocrystals, Polym. Adv. Technol. 32 (2021) 76–86, https://doi.org/10.1002/pat.5062.

[41] M. Zakizadeh, M. Nourany, M. Javadzadeh, P.Y. Wang, H. Shahsavarani, Analysis of crystallization kinetics and shape memory performance of PEG-PCL/MWCNT based PU nanocomposite for tissue engineering applications, Express Polym Lett 15 (2021) 418–432, https://doi.org/10.3144/expresspolymlett.2021.36.

[42] M.D. Ries, L. Pruitt, Effect of cross-linking on the microstructure and mechanical properties of ultra-high molecular weight polyethylene, Clin. Orthop. Relat. Res. 440 (2005) 149–156, https://doi.org/10.1097/01.blo.0000185310.59202.e5.

[43] X. Yu, B.P. Grady, R.S. Reiner, S.L. Cooper, Mechanical and thermal properties of UV-curable polyurethane and polyurea acrylates, J. Appl. Polym. Sci. 49 (1993) 1943–1955, https://doi.org/10.1002/app.1993.070491110.

[44] K.H. Lee, B.K. Kim, Structure-property relationships of polyurethane anionomer acrylates, Polymer (Guildf.) 37 (1996) 2251–2257, https://doi.org/10.1016/0032-3861(96)85871-X.

[45] S. Murali, A. Agirre, L. Irusta, A. González, R. Tomovska, Chemical structure of zwitterionic monomers as a tool to produce colloidally stable (meth)acrylic polymer colloids, Polymer (Guildf.) (2023) 126421, https://doi.org/10.1016/j.polymer.2023.126421.